CHAPTER 9

PHYSICAL AND PHYSICOCHEMICAL RATE PROCESSES

9.1 INTRODUCTION

Physical processes are an important part of microelectronics processing. In general, much of metallization and dielectric material deposition is still carried out either by direct evaporation of a source solid (for deposition on a substrate) or by physical sputtering. Deposition based on the evaporation of a source solid(s) is sometimes referred to as physical vapor deposition (PVD), as opposed to chemical vapor deposition. Physical sputtering is a process in which ions accelerated by an applied electric field sputter (eject) atoms from a substrate surface by momentum transfer. As such, physical sputtering can be used for both etching and deposition: etching if the substrate is the target and deposition if it receives sputtered atoms from a target. An important application of evaporation is the technique known as molecular beam epitaxy (MBE). MBE is primarily used for compound semiconductors because of its ability to deliver well-defined thin-film layers at relatively low temperatures, which in turn allows for well-defined doping profiles.

Plasma processes are becoming more versatile and useful for device fabrication. Although physical sputtering processes (in which the ions are generated) may also involve plasmas, the term plasma process is usually reserved for one in which chemical processes eventually get involved in deposition or etching. The origin of the chemical activity, however, is the physical process in which reactive neutral species (or ions) are generated in a plasma by electrons colliding with

molecules. Therefore, plasma processing is governed by physicochemical rate processes. The major impetus for plasma processing is the low-temperature environment that the plasma offers. Further, anisotropy can be realized much more easily by plasma etching than by any other etching technique due to the normal incidence of ions onto the substrate. Substrate surface modification through momentum transfer by colliding ions is a major reason for the enhanced etching by reactive species in the plasma. Because a plasma is formed when an electric field is applied between two electrodes or by an alternating voltage, electrical characteristics of the plasma process are one of the major factors, if not the sole factor, that govern the plasma process.

In this chapter, PVD (physical vapor deposition) is treated first. Since plasma is central to the rest of the chapter, the nature and characteristics of plasma are then treated for subsequent sections of physical sputtering, plasma deposition, and plasma etching.

9.2 EVAPORATION AND PHYSICAL VAPOR DEPOSITION

Evaporation in vacuum from free solid surfaces is often used to deposit metal for device interconnections. The evaporation is also used to deposit epitaxial films, better known as molecular beam epitaxy (MBE). The source solid is heated by resistance or induction heating (with a crucible that couples with the rf) and the evaporated molecules then deposit by condensation onto the cold surface of the substrate. The source solid can also be bombarded by a particle beam (electron or ion) to generate the vapor. Conventional sputtering, which involves acceleration of ions (usually Ar^+) through a potential gradient and the bombardment by these ions of a target or cathode, is another form of physical vapor deposition. Through momentum transfer, atoms near the surface of the target material become volatile and are transported as a vapor to the substrate.

The quantities of interest are the rates of evaporation and deposition. The latter depends strongly on the directionality of motion of evaporating molecules. The driving force for the evaporation is the saturation vapor pressure, p^*, on the solid surface that must be maintained at a given temperature. Counteracting the driving force is the rate of impingement (adsorption) from the vapor phase to the solid. Thus, the net number of molecules dN evaporating from a solid surface area A during the time dt is given by

$$\frac{dN}{A\,dt} = (2mk_B T)^{-1/2}(p^* - p) \tag{9.1}$$

where k_B is the Boltzmann constant, T is temperature, m is the mass of the molecule, p is the partial pressure of the evaporant in the gas phase, and p^* is the corresponding equilibrium pressure. The relationship is known as the Hertz-Knudsen equation (Glang, 1970) when the right-hand side of the equation is multiplied by a constant called the evaporation coefficient, which is less than unity. The maximum rate of evaporation, which is the rate for unit evaporation

coefficient and zero pressure, is often used to represent the mass rate of evaporation V as follows:

$$V[g/(cm^2 \cdot s)] = 5.834 \times 10^{-2}\left(\frac{M}{T}\right)^{1/2} p^* \tag{9.2}$$

where M is the molecular weight and p^* is in torr. The total mass evaporation rate is that obtained by integrating over the solid surface area A:

$$V_t\,(g/s) = \int_A V\, dA \tag{9.3}$$

The direction in which molecules will be emitted from a solid surface can be modeled by considering the interaction between the solid surface and an individual molecule about to evaporate. Consider an isothermal enclosure with an infinitesimally small opening dA_e bounded by vanishingly thin walls as shown in Fig. 9-1. It can be shown (Glang, 1970) that the differential total mass rate of evaporation is given by

$$dV_t(\Omega) = V_t \cos \Omega \frac{d\omega}{\pi} \tag{9.4}$$

Since $dA_r = r^2\, d\omega/\cos \alpha$ according to the geometry in Fig. 9-1, one has, from Eq. (9.4),

$$\frac{dV_t}{dA_r} = \frac{V_t}{\pi r^2} \cos \Omega \cos \alpha = r_D \tag{9.5}$$

where r_D (mass per area per time) is the maximum rate of deposition and r is the distance between the source and substrate. This relationship is known as the

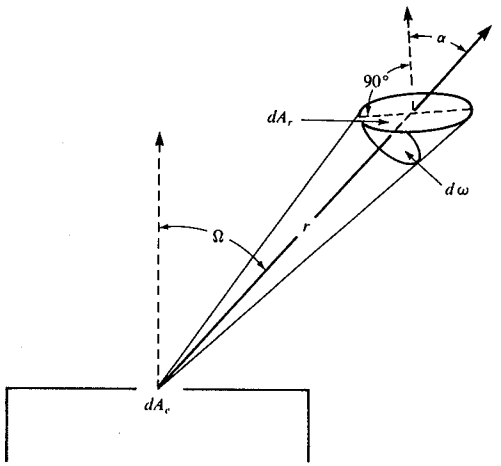

FIGURE 9-1
Surface element dA_r receiving deposit from a small area source (Glang, 1970).

cosine law of emission. The extension of this cosine law to emission from solid surfaces is generally taken to be permissible. For a point source, although of limited practical utility, Eq. (9.5) reduces to

$$\frac{dV_t}{dA_r} = \frac{V_t \cos \alpha}{\pi r^2} \tag{9.6}$$

The deposition rate at various points on a substrate plane above a small area source [Eq. (9.5)] can be expressed (Chang, 1970) as

$$\frac{r_D}{(r_D)_0} = \left[1 + \left(\frac{L}{r}\right)^2\right]^{-2} \tag{9.7}$$

where $(r_D)_0$ is the rate directly above the source at a distance r and r_D is the rate at the point L away from the center of the substrate plane. Likewise, one has, for a point source [Eq. (9.6)],

$$\frac{r_D}{(r_D)_0} = \left[1 + \left(\frac{L}{r}\right)^2\right]^{-3/2} \tag{9.8}$$

When the receiving surface is spherical with a radius of r_0, as shown in Fig. 9-2, $\cos \alpha = \cos \Omega = r/2r_0$ and Eq. (9.5) can be rewritten as

$$r_D = \frac{V_t}{4\pi r_0^2} \tag{9.9}$$

It is seen that the maximum deposition rate is the same everywhere on the spherical surface. This is the reason why planetary substrate-supporting systems (rotating spherical sections) are used in deposition chambers.

Example 9.1. At 3230 °C, the saturation pressure of tungsten (mp = 3380 °C) is 0.01 torr. Calculate the mass rate of evaporation. Assume the source area to be 1 cm² and the evaporation chamber pressure to be 10^{-4} torr. Also calculate the maximum

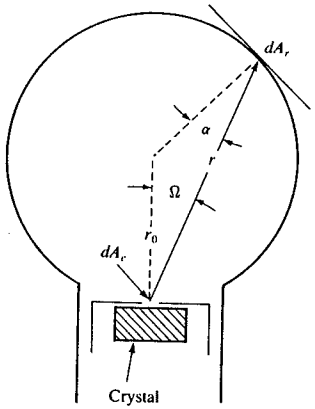

FIGURE 9-2
Evaporation from a small area source dA_e onto a spherical receiving surface (Glang, 1970).

rate of deposition on a substrate placed directly above and 2 cm away from the metal source. Determine the maximum deposition rate for a substrate 5 cm away from the center of the substrate plane.

Solution. The mass rate is given by Eq. (9.2):

$$V = 5.834 \times 10^{-2}\left(\frac{183.85}{3503}\right)^{1/2} \times 0.01$$

$$= 1.337 \times 10^{-4}\ \text{g/(cm}^2\cdot\text{s)}$$

For the source area of 1 cm^2, $V_t = 1.337 \times 10^{-4}$ g/s. For the substrate placed directly above the source, $\cos\alpha = \cos\Omega = 1$. Thus, one has, from Eq. (9.5),

$$r_D = \frac{V_t}{\pi r^2} = \frac{1.337 \times 10^{-4}}{3.14(2)^2} = 1.06 \times 10^{-5}\ \text{g/(cm}^2\cdot\text{s)}$$

Noting for the last part of the problem that $(r_D)_0 = 1.06 \times 10^{-5}$ g/(cm^2·s), one has, from Eq. (9.7),

$$r_D = (r_D)_0\left[1 + \left(\frac{L}{r}\right)^2\right]^{-2}$$

$$= 1.06 \times 10^{-5}[1 + (\tfrac{2}{3})^2]^{-2}$$

$$= 0.788 \times 10^{-5}\ \text{g/(cm}^2\cdot\text{s)}$$

Physical vapor deposition (PVD) occurs when evaporated source material is condensed onto a surface (substrate surface) that is cold relative to the evaporating surface. For silicon epitaxy by MBE, for example, the cold surface temperature ranges from below 800 to 850 °C; it is around 500 °C for GaAs. As in CVD film growth, the growth by PVD involves condensation of atoms (adatoms), subsequent migration of the adatoms on the surface, and incorporation of the adatoms into a crystal structure. The major difference is that PVD involves condensation (physical adsorption in a broad sense) whereas CVD involves mostly chemical adsorption. The consequence of this difference is that both adsorption and desorption have to be considered for the kinetics of CVD whereas only condensation onto a cold surface is needed in PVD. The type of crystal structure that results from PVD is entirely determined by the relative rate of condensation with respect to the rate of adatom migration. If the condensation rate is much higher than the surface migration rate, an amorphous structure would result, which is typical of the metallization by PVD. On the other hand, a single crystalline structure would result if the condensation rate is less than or equal to the (potential) rate of surface migration at a given temperature, as in the case in MBE. A polycrystalline structure forms in between these two extremes. Therefore, it is natural that the rate of deposition is the same as the net rate of condensation (often called the rate of impingement) when an amorphous structure is involved. Noting that the condensation rate is the limiting process in epitaxial deposition, one can conclude the same is true for epitaxial deposition. Therefore, it is sufficient to consider only the condensation rate in determining

the rate of deposition. Neglecting reevaporation of the condensed phase from the relatively cold surface gives a net rate of condensation:

$$r_c = (2mk_B T)^{-1/2}p^*$$

$$= 3.513 \times 10^{22}(MT)^{-1/2}p^* \qquad (9.10)$$

where M is the molar mass in grams and p is in torr.

Example 9.2. Meyerson *et al.* (1986) used a low-pressure (10^{-3} torr) CVD to deposit epitaxial silicon film on a silicon wafer at temperatures ranging from 750 to 850 °C. The average growth rate was reported to be 6 nm/min. Noting that the temperature range is similar to that for the MBE of silicon and that the growth rate can be used as that sustainable in the MBE, calculate the maximum pressure that can be allowed for film growth by MBE. Assume the gas temperature to be at 800 °C.

Solution. Since Eq. (9.10) is in atoms per square centimeter per second, the linear growth rate of 6 nm/min needs to be converted to the following:

$$\frac{G\rho_s N_A}{M_s} = \frac{(6 \times 10^{-7}/60)(2.33)(6.02 \times 10^{23})}{28}$$

$$= 5.01 \times 10^{14}\ \text{atoms/(cm}^2\cdot\text{s)}$$

where G is the linear growth rate, ρ_s and M_s, respectively, are the silicon density and molecular weight, and N_A is Avogadro's number. For epitaxy by MBE, the condensation rate given by Eq. (9.10) should be less than or equal to the growth rate given in Example 9.1:

$$3.513 \times 10^{22}(MT)^{-1/2}p \le 5.01 \times 10^{14}$$

or

$$p\ (\text{torr}) \le 2.47 \times 10^{-6}$$

As the example illustrates, the pressure required for MBE is much lower than that for CVD epitaxy, because the impingement rate cannot be larger than the maximum possible rate of epitaxial growth at a given temperature. This in turn means that the pressure for epitaxy by PVD should be very low but that the pressure for metallization (amorphous structure) can be relatively much higher. Typical pressures for silicon MBE are 10^{-8} torr, while those for metallization are in the 10^{-3} to 10^{-8} to 10^{-10} torr range. Impingement rates for a number of evaporants and background residual gases are given in Fig. 9-3. The broken lines in the figure indicate that a chromium condensation rate of 1 Å/s corresponds to 8×10^{14} atoms/(cm^2·s). It is necessary to minimize any residual gas species in the evaporation chamber, since they also deposit. As shown in Fig. 9-3, an oxygen partial pressure of 10^{-6} torr would result in an incorporation of oxygen at a competing rate of 4×10^{14} molecules/(cm^2·s). In contrast, a dopant source can be introduced to the chamber as the desired impurity for doping.

The relatively high temperature of the cold substrate surface has an important bearing on the defect level of an epitaxial film. The dislocation density of an MBE silicon decreases with increasing temperature, as shown in Fig. 9-4. This is

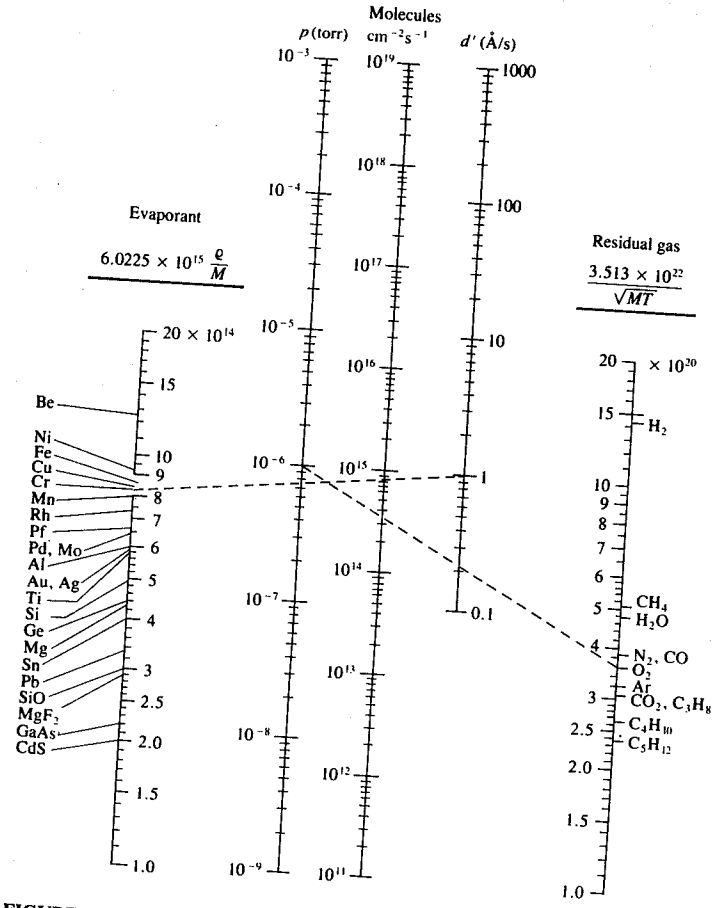

FIGURE 9-3
Nomogram to determine impingement rate. The appropriate point in the evaporant axis is to be connected with the observed (pure) deposition rate on the d' axis. For residual gases, points on the far right and on the pressure axes should be connected. The intersects with the center axis give the impingement rates (Glang, 1970).

expected since the surface migration rate increases with increasing temperature while the impingement rate decreases to some extent. One would also expect the defect level to decrease with decreasing pressure because of the corresponding decrease in the impingement rate, which favors more orderly epitaxial growth.

Vaporization of solid substances can also be caused by electron bombardment of the substance surface. The electron source is usually a hot cathode. The

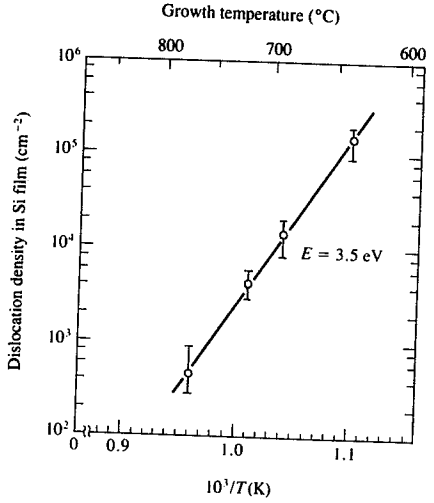

FIGURE 9-4
Temperature dependence of dislocation density (Sugiura and Yamaguchi, 1980).

electrons are accelerated through fields of 5 to 10 kV onto the evaporant surface. Since the energy is imparted by charged particles, only the surface is heated. The surface temperature can exceed 3000 °C (Glang, 1970) while the remainder of the solid is maintained at a lower temperature. Devices operating on the principle of electron-bombardment heating are referred to as electron guns. While solid substances have been the major evaporant, vapor substances are increasingly used in MBE, in particular for III-V compounds films (Cho, 1987).

Another major method of metallization for VLSI circuits is physical sputtering. An understanding of plasmas, however, is required to go into the sputtering.

9.3 PLASMA

A plasma is a collection of positively and negatively charged particles, including neutral ones. Charge neutrality requires that the number density of the positive charges is equal to that of the negative ones. Plasma constitutes the fourth state of matter. As a matter is heated, its state changes from solid to liquid, from liquid to gas, and then to plasma. The plasma state is in fact by far the most common form of matter (up to 99 percent of the universe). It is also the most energetic state: matter requires on the average 10^{-2} eV/particle to change its state from solid to liquid or from liquid to gas, but it requires 1 to 30 eV/particle to change its state from gas to plasma.

The essence of plasmas as applied to film deposition and etching lies in a self-sustaining discharge between cathode and anode, in particular glow discharge. Three types of self-sustaining discharges can result when electrons are emitted from a cathode (discharge). These are dark discharges, gas discharges,

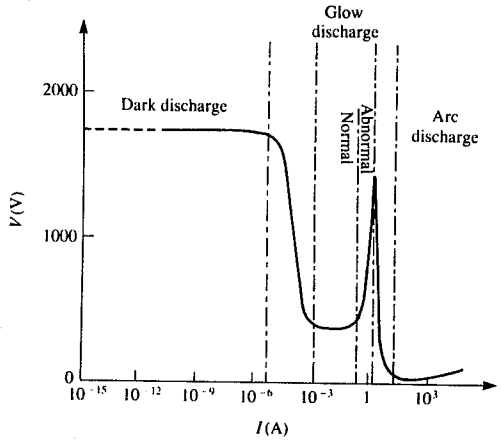

FIGURE 9-5
Current-voltage characteristic in a self-sustaining discharge (Kettani and Hoyaux, 1973).

and arc discharges. The types are determined by the current-voltage characteristics of the discharge as shown in Fig. 9-5. A current will flow between the separated electrodes in a gas at low pressure, provided the applied voltage is above the minimum, or breakdown, voltage. The breakdown voltage is that level at which the gas can be at least partially converted to plasma. As the electrons emitted from the cathode travel toward the anode, they make a fixed number of ionizing collisions. The ions that result from these collisions are also accelerated by the applied field and move toward the cathode. Some of these ions, on striking the cathode, eject secondary electrons from its surface. The glow that results is said to be self-sustained when the number of secondary electrons produced at the cathode is sufficient to maintain the discharge.

A self-sustained glow discharge has a fair degree of structure that is visible, as illustrated in Fig. 9-6. The Crookes dark space is where positive ions have accumulated. The dark space adjacent to an electrode (cathode) is often referred to as a plasma sheath or simply a sheath. Its thickness is approximately the mean distance traveled by an electron from the cathode before it makes an ionizing collision. Electrons traverse the dark space very rapidly because of the localized

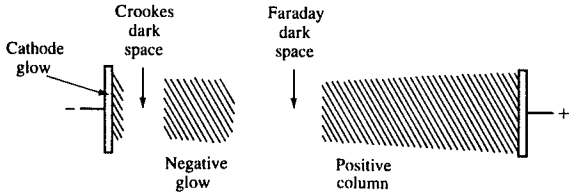

FIGURE 9-6
Cross-sectional view of glow discharge (Maissel, 1970).

space charge there. As the edge of the negative glow is reached, electrons begin to produce a significant number of ion-electron pairs, and the preponderance of the positive charge falls off very rapidly. A neutral region consisting of approximately equal numbers of ions and electrons begins, forming a plasma. At relatively low voltages the cross-sectional area of the glow is less than the available cathode area since there exists a minimum current density requirement for maintaining the glow. If additional power is applied to the discharge tube, the glow adjusts by increasing its cross-sectional area, thus raising the total current but keeping the current density at the cathode constant. As long as this current density does not increase, neither does the voltage across the dark space. The minimum voltage drop needed to maintain the glow is called the normal cathode fall, and the corresponding glow is referred to as the normal glow. When the power is increased beyond the point where the glow covers the entire available cathode area, the current density at the cathode must increase. This in turn implies an increase in the emission of secondary electrons from the cathode. The glow discharge operating in this mode is referred to as abnormal (Fig. 9-5). In practice, this is the only mode of interest for film deposition by physical sputtering. The current density in the normal glow is too low for atoms to be sputtered out of the cathode at a useful rate. At the same time, the corresponding voltage drop is quite low (Fig. 9-5) so that sputtering yields are similarly low.

When electrons enter the negative glow, they possess essentially the full cathode fall of potential. This energy is then lost through a series of either ionizing or excitation collisions. Eventually, the electrons' energy is reduced to a point where they are no longer able to produce additional ions. The region in the discharge where this happens defines the far edge of the negative glow, and since no more ions are being produced, the electrons begin to accumulate there, forming a region of slightly negative space charge. In this region, the electrons have insufficient energy to cause either ionization or excitation. Consequently, it is a dark region, known as the Faraday dark space. After passing through the Faraday dark space by diffusion, electrons are accelerated toward the anode. This region is called the positive column.

Since the self-sustaining feature of the discharge depends only on the emission of sufficient electrons at the cathode by positive ions from the negative glow, the exact location of the anode normally makes very little difference to the electrical characteristics of the glow. Thus, if the anode is moved closer and closer in toward the cathode, the positive column will be extinguished, the Faraday dark space will disappear, and, finally, a large fraction of the negative glow may be extinguished before any appreciable effect is seen in the electrical characteristics.

If an electrode is inserted into a glow and is biased with respect to the anode, the effect of negative bias is that a second cathode is created with its own ion sheath around it. However, since the flow is already being sustained by the flow of secondary electrons from the primary cathode, the second cathode can operate at as low a voltage as desired since the glow is not dependent on it for a supply of secondary electrons. The additional cathode is referred to as a probe. More details can be found in Maissel (1970).

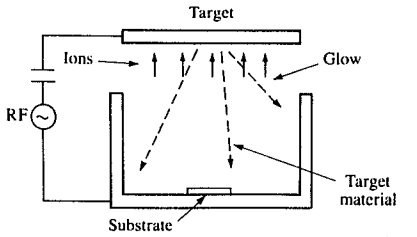

(*a*) Sputter deposition

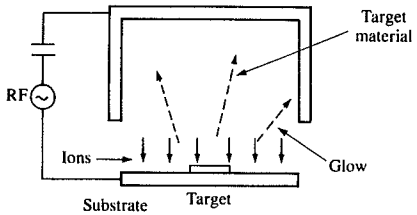

(*b*) Sputter etching

FIGURE 9-8
Two modes of operation of a two-electrode rf sputtering system (Horwitz, 1983).

where $$\alpha = \frac{5.2}{U}\frac{Z_t}{(Z_t^{2/3} + Z_x^{2/3})^{3/4}}\left(\frac{Z_x}{Z_t + Z_x}\right)^{0.67}$$

E is the ion energy in kiloelectronvolts, E_{th} is the threshold energy in kiloelectronvolts, U is the surface binding energy in electronvolts, which can be taken as the sublimation energy, and Z_t and Z_x, respectively, are the atomic numbers of the target and the gas. When the gas is a molecule consisting of m atoms, the relationship becomes

$$S = m^{1/2}\alpha[E^{1/2} - (mE_{th})^{1/2}] \tag{9.12}$$

Example 9.3. Consider tungsten deposition in a dc discharge with Ar. The threshold energy is 33 eV. Calculate the sputtering yield for a cathode voltage of 100 volts. The heat of sublimation of tungsten is 191 kcal/mol. Use the sheath potential (voltage drop across the sheath) for the cathode potential. Note that 1 kcal/mol is equal to 0.0434 eV/molecule.

Solution. The ion energy is 100 eV for the cathode potential of 100 volts. Also, from the sublimation energy,

$$U = 0.0434 \times 191 = 8.29 \text{ eV/molecule (atom)}$$

For the target tungsten and the gas Ar,

$$Z_t = 74 \quad \text{and} \quad Z_x = 18$$

These values can be used in Eq. (9.11) for α:

$$\alpha = \frac{5.2}{8.29}\frac{74}{(74^{2/3} + 18^{2/3})^{3/4}}\left(\frac{18}{74 + 18}\right)^{0.67} = 1.41$$

and thus one has for the sputtering yield

$$S = 1.41(0.1^{1/2} - 0.033^{1/2})$$
$$= 0.19 \text{ atom/ion}$$

The experimental value for the yield (Wehner and Anderson, 1970) is 0.1 atom/ion.

The rate of sputtering, r_s, which can be defined as the number of atoms sputtered per unit time per unit area, can be obtained by multiplying the sputtering yield by the ion flux. Since ion current density (current flux) is equal to the ion flux times electron charge q, one has, for r_s,

$$r_s = \frac{Sj_i}{q} \tag{9.13}$$

where j_i is the ion current density. Although the rate of sputtering is given by Eq. (9.13), it is not a simple matter to relate the ion energy and the ion current density to pertinent electrical and physical characteristics of sputtering.

For deposition by physical sputtering, the pressure is usually low enough that collisions in the target sheath can be neglected. Under the "space charge limited condition," the ion current density can be expressed (Hasted, 1964) as

$$j_i = \frac{\beta V_{sp}^{3/2}}{d^2 M_i^{1/2}} \tag{9.14}$$

where β is a constant, which is equal to $0.85p_0 q^{1/2}$ where p_0 is the permittivity of free space, V_{sp} is the sheath potential (voltage drop across the dark space adjacent to the cathode in dc sputtering and adjacent to the powered electrode in the case of rf sputtering), d is the sheath thickness, and M_i is the ion mass. For dc glow discharges, the sheath potential can be taken as the voltage applied to the cathode or the cathode potential. However, the situation is more complicated for rf discharges.

Example 9.4. The electrical quantities that are readily measurable in the dc sputtering are the cathode potential and the cathode current. Although the cathode current is mainly by ions, the secondary electrons emitted from the cathode by the incident ions do contribute to the current. If the number of secondary electrons emitted per incident ion is denoted by μ, the cathode current density j_c can be expressed (Brown, 1966) as

$$j_c = j_i(1 + \mu)$$

A typical number for μ is 0.1. Consider in this light tantalum deposition by dc sputtering as reported by Vratny (1967). The deposition rate reported is 8 nm/min with a cathode potential of 850 volts, and the corresponding cathode current density

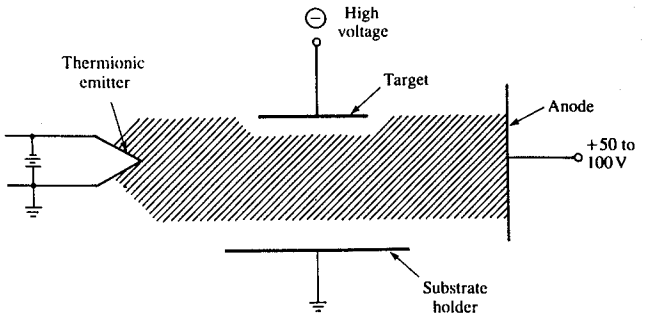

FIGURE 9-7
Schematic of thermionically supported glow discharge adapted for sputtering (triode sputtering) (Maissel, 1970).

The simplest discharge is the one produced by applying a dc potential between two metal electrodes in a partially evacuated enclosure. Typically, the discharge operates at pressures exceeding 3×10^{-2} torr and the applied voltage exceeding a few hundred volts. Instead of electrons by secondary emission, a hot cathode can be used to supply the electrons through thermionic emission, sometimes called a low-voltage arc. Such a system can provide finite current even at pressures lower than 3×10^{-2} torr. At still lower pressures ($\sim 10^{-3}$ torr), the mean free path for electrons exceeds the typical dimensions of discharge enclosure, and the probability of ionizing collisions is too small to maintain the discharge unless the electrons are confined by an external magnetic field (Bollinger and Fink, 1980) or by insertion of a probe (target), as shown in Fig. 9-7.

Suppose that an alternating voltage is applied to the two electrodes instead. At sufficiently low frequencies a dc discharge can be produced that alternates between the two electrodes at the same frequency. On the other hand, no dc discharge can be established if the frequency is high. The discharge simply oscillates between the electrodes and the electrons pick up sufficient energy during their oscillations (random motion) to cause ionization. The minimum pressure at which the discharge will occur is gradually reduced with increasing frequency. The frequency at which such a discharge is sustainable is usually in the radio-frequency (rf) range, the effect being detectable above about 50 kHz and leveling off for frequencies in excess of a few megahertz. This mode of discharge is referred to as rf discharge.

The rf discharge is the main method of producing a plasma in applications to IC processing because of several advantages it can offer. First, sputtering of an insulator is possible with an rf discharge. Simple substitution of an insulator for the metal target in dc discharge leads to failure because of the immediate buildup of a surface charge of positive ions on the front side of the insulator, preventing

any further ion bombardment. This also permits the use of reactive gases typically used in plasma etching since the electrodes within the discharge can be covered with insulating material. Second, the rf discharge can be operated at pressures as low as 10^{-3} torr, where the mean free path of ions and of sputtered atoms become comparable with or larger than the enclosure dimensions. This reduces or eliminates many of the complications inherent in glow discharges such as diffusion of sputtered material back to the target, poorly defined bombarding-ion energies, charge exchange effects, etc. Third, the discharge can be sustained independently of the yield of secondary electrons from the walls and electrodes.

Low-pressure plasmas used in IC processing are generally characterized by a low degree of ionization (typically 0.1 to 1 percent) and an absence of thermal equilibrium between ions, electrons, and neutral gas molecules. The range of electron energies is between 1 and 20 eV. The ion densities are normally between 10^9 and 10^{12} cm^{-3}. This is set by fundamental limits. When the density is less than 10^9 cm^{-3}, the electrostatic force is weak enough for the charge to separate over a fairly large distance and neutrality is no longer maintained. This is usually unstable as an operating region. Plasma densities higher than 10^{12} cm^{-3} correspond to high currents and significant gas heating. High temperature can be harmful to substrate materials and leads to plasma instability and nonuniformity (Flamm and Herb, 1988). Considering that the density of gas molecules at 1 torr is about 10^{16} cm^{-3}, it can be seen that the discharges are weakly ionized. This results in a nearly ambient gas temperature, despite a mean electron temperature of about 10^4 to 10^5 K. The relatively low gas temperature permits the use of thermally sensitive materials such as organic resists.

Physical sputtering based on plasma can be used for both deposition and etching. In the case of deposition, the atoms sputtered out by the target (cathode) deposit onto a substrate as shown in Fig. 9-8. If the target itself is the substrate as shown in Fig. 9-8*b*, the sputtering results in etching of the substrate. The deposition is usually referred to as physical sputtering, although physical sputtering can also be used for etching as in ion milling (Bollinger and Fink, 1980).

9.4 PHYSICAL SPUTTERING

Two key quantities of interest in physical sputtering are the threshold energy and the sputtering yield. The threshold energy is defined as the minimum ion energy for sputtering to ensue from a target bombarded at normal incidence by an ion. The threshold energies for various metals with noble gases can be found in Wehner and Anderson (1970). The threshold values are roughly four times the metal sublimation energy for most inert gases used for physical sputtering. The sputtering yield is defined as the number of target atoms sputtered by one colliding ion. The sputtering yield S in the energy range of interest for film deposition (a few hundred to a few kiloelectronvolts) can be determined theoretically (Steinbruchel, 1985) from

$$S = \alpha(E^{1/2} - E_{th}^{1/2}) \tag{9.11}$$

is 0.25 mA/cm² in an argon environment of 20 millitorr. Calculate the rate of sputtering, and compare it with the reported deposition rate. The heat of sublimation of Ta is 190 kcal/mol and the threshold energy is 26 eV. Discuss the results.

Solution. From the latent heat of sublimation,

$$U = 0.0434 \times 190 = 8.25 \text{ eV/atom}$$

For the target of tantalum and the gas Ar,

$$Z_t = 73 \quad \text{and} \quad Z_x = 18$$

As in Example 9.3, one can calculate α; it is 1.4. From Eq. (9.11),

$$S = 1.4(0.85^{1/2} - 0.026^{1/2})$$

$$= 1.065 \text{ atom/ion}$$

Since $j_c = j_i(1 + \mu)$ and $j_c = 2.5 \times 10^{-4}$ A/cm², one has, for μ of 0.1,

$$j_i = \frac{j_c}{1 + \mu} = \frac{2.5 \times 10^{-4}}{1.1} = 2.273 \times 10^{-4} \text{ A/cm}^2$$

From Eq. (9.13) for r_s,

$$r_s = \frac{1.065 \times 2.273 \times 10^{-4}}{1.6 \times 10^{-19}} = 1.51 \times 10^{15} \text{ atoms/(s·cm}^2\text{)}$$

To convert from a linear deposition rate (G) of 8 nm/min or 0.133 nm/s, one can use the following:

$$r_d \text{ [atoms/(s·cm}^2\text{)]} = \frac{G\rho N_A}{M}$$

$$= \frac{(0.133 \times 10^{-7})(16.6)(6.02 \times 10^{23})}{181}$$

$$= 7.34 \times 10^{14}$$

where ρ and M, respectively, are the density and atomic weight of tantalum and N_A is Avogadro's number.

The results show that the actual rate of deposition is approximately one half the rate of sputtering. Aside from the numbers, it should be understood that the actual rate of deposition is generally smaller than the intrinsic rate of sputtering, because of the effects involved in the transport of the sputtered atoms to the substrate located on the anode. The sputtered atoms can also deposit onto surfaces other than the substrate such as walls. On the other hand, the rate of etching is the same as the rate of sputtering, since then the target, substrate, is itself.

Consider rf discharge for the ion energy. Radio-frequency discharges consist of two parts, as shown in Fig. 9-9. These are the plasma body which has approximately equal numbers of electrons and ions and the two sheaths, one at each electrode, where the ion density is much larger than the electron density. Shown

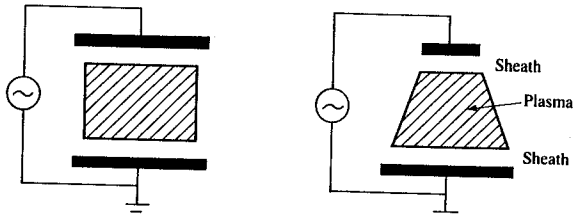

(*a*) Symmetric (*b*) Asymmetric

FIGURE 9-9
Symmetrical and asymmetrical electrode systems.

in Fig. 9-9*a* is the case where the powered electrode area (A_p) is the same as the grounded electrode area (A_g); Fig. 9-9*b* is for $A_g > A_p$. The former is referred to as a symmetrical electrode system; the latter is called asymmetrical. In the plasma sheaths, the current is dominated by ions. Further, no secondary electrons from the target are involved in maintaining the plasma. Therefore, the root mean square current measured at the powered electrode can be taken as the ion current density (when it is divided by A_p), j_i. In the plasma, however, electrons dominate as the major current carriers because of their higher mobility compared with the ions, even though the electron density is approximately equal to the cation density.

The plasma of an rf discharge develops an appreciable potential, V_p, which is positive with respect to both electrodes. This is shown in Fig. 9-10 for both symmetrical and asymmetrical cases. In the symmetric electrode system, the sheath potential V_{sp} is the same at both electrodes and is equal to the plasma potential V_p. Therefore, the average ion energy is that corresponding to V_p.

In the asymmetrical case, however, the current density varies because the electrode areas are different and yet the current is the same at both electrodes. This difference causes a bias of voltage at the powered electrode (small area). This is shown in Fig. 9-10*c* for time-varying voltage distributions. Note in this regard

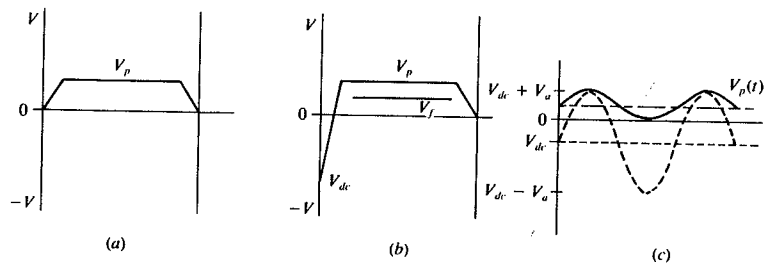

FIGURE 9-10
Voltage characteristics of symmetrical and asymmetrical electrode systems.

that the voltage distributions in Fig. 9-10*a* and *b* are for the time-averaged values. However, rf systems without a blocking capacitor do not have bias regardless of the area ratio. The average plasma potential can be determined (Chapman, 1980) from

$$V_p = 0.5(V_a + V_{dc}) \tag{9.15}$$

where V_a is the applied voltage amplitude (Fig. 9-10*c*). In a capacitively coupled rf discharge, the sheath potential is given (Coburn and Kay, 1972) by

$$V_{sp} = V_p - V_{dc} \tag{9.16}$$

Note that the reference voltage is the ground, such that the value of V_{dc} is negative.

Example 9.5. Consider an rf discharge operating at 13.56 MHz. Many rf discharge processes operate at this frequency because it is the one allotted to international communications. For an asymmetrical, parallel-plate system, suppose that the root mean square current and applied voltage amplitude are 0.1 ampere and 160 volts, respectively, and that the powered electrode area is 10 cm^2 whereas the grounded electrode area is 30 cm^2. The dc bias with respect to the ground is 80 volts. Calculate the aluminum sputtering rate for an aluminum target placed on the powered electrode in an argon environment. For aluminum, the threshold energy in argon is 13 eV/atom and the latent heat of sublimation is 3.25 eV/atom. Recalculate the rate for the case where the target is placed on the grounded electrode.

Solution. The sheath and plasma potentials follow from Eqs. (9.15) and (9.16):

$$V_p = 0.5(160 - 80) = 40 \text{ volts}$$

$$V_{sp} = 40 - (-80) = 120 \text{ volts}$$

Since ions dominate in the sheath, the ion current density at the powered electrode can be calculated as follows:

$$j_i = \frac{0.1}{10} = 0.01 \text{ A/cm}^2$$

The sputtering yield can be calculated from Eq. (9.11):

$$\alpha = \frac{5.2}{3.25}\frac{13}{(13^{2/3} + 18^{2/3})^{3/4}}\left(\frac{18}{13 + 18}\right)^{0.67} \qquad \text{for } Z_{Al} = 13$$

$$= 2.257$$

$$S = 2.257(0.12^{1/2} - 0.013^{1/2}) = 0.52 \text{ atom/ion}$$

since the ion energy is that corresponding to the sheath potential. The rate of sputtering follows directly from Eq. (9.13):

$$r_s = \frac{0.52(0.01)}{1.6 \times 10^{-19}}$$

$$= 3.25 \times 10^{16} \text{ atoms/(cm}^2\text{·s)}$$

If the target is placed on the grounded electrode, the ion energy is that corresponding to V_p, or 40 eV. The current density is

$$j_i = \frac{0.1}{30} = 0.0033 \text{ A/cm}^2$$

The sputtering yield is

$$S = 2.257(0.04^{1/2} - 0.013^{1/2}) = 0.194 \text{ atom/ion}$$

Thus,

$$r_s = \frac{0.194(0.0033)}{1.6 \times 10^{-19}}$$

$$= 4 \times 10^{15} \text{ atoms/(cm}^2\text{·s)}$$

This example shows that the intrinsic rate of sputtering, which is the maximum possible rate of deposition in the case of film deposition and the actual rate of etching in the case of etching, is much higher when the target is placed on the powered electrode than on the grounded electrode. Therefore, the asymmetrical system is usually used in rf sputtering and the area ratio, A_p/A_g, is an important design parameter. Since the rate of sputtering is entirely determined by ion energy and current density, it is necessary to relate these to the transport processes of electrons and ions in the sputtering apparatus. This is treated in the next chapter.

As discussed earlier, a simple substitution of an insulator for the metal target fails in a conventional dc sputtering system because of the immediate buildup of a surface charge of positive ions on the front side of the insulator. This prevents any further ion bombardment. However, in rf sputtering, the voltage alternates so that the target is alternately bombarded by cations and then electrons, which dissipates the charge buildup. Therefore, rf sputtering is the method of choice for both insulator etching and deposition.

An important feature of the sputtering process (Maissel, 1970) is that the chemical composition of a sputtered film is often the same as that of the target from which it was sputtered. This is true even though the components of the system may differ significantly in their relative sputtering rates, except when resputtering occurs. The very first time that sputtering is performed from a multicomponent target, the component with the highest sputtering rate comes off faster, but a so-called "altered region" soon forms at the surface of the target. This region becomes depleted in the higher sputtering rate component to compensate for its greater removal rate and later sputtering rates tend to even out. Subsequent deposits have the composition of the parent material. However, the stoichiometry of a film obtained from a compound material is not the same as the parent material. In this case, the target is sputtered both in the molecular and atomic forms (Coburn *et al.*, 1974). Often the film is deficient in gaseous or other volatile species. For example, an oxide film obtained by sputtering can be deficient in oxygen.

Example 9.6. Consider the example by Chapman (1980) for the sputtering of a 80:20 Ni-Fe alloy. For 1000-eV argon ions, the sputtering yield is 2.1 for Ni and 1.4 for Fe. After the initial period, the composition of the alloy film should be in the ratio of 80:20. Determine the composition of the target surface that would yield the desired film composition.

Solution. The initial ratio of the sputtered atoms will be $(80 \times 2.1):(20 \times 1.4)$. As the iron enrichment continues, the sputtering rate of the iron atoms increases and of nickel atoms decreases until they are again leaving in the ratio 80:20. For the ratio of sputtered atoms to be 80:20, the following condition has to be satisfied:

$$\frac{2.1y}{1.4(1-y)} = \frac{80}{20}$$

where y is the fraction of Ni in the target surface after the initial period. The solution yields a value of 0.727 for y, meaning that the surface composition is 72.7 percent Ni and 27.3 percent Fe.

The deficiency in the stoichiometry of a deposited compound film can be compensated for by introducing a gas containing the deficient atoms, deficient gas, in the sputtering environment. For example, any oxygen deficiency in the deposited film can be corrected by introducing a suitable amount of oxygen to the gaseous environment such as argon (Erskine and Cserhati, 1978). This is turn means that any undesired impurities in the environment will also deposit onto the film. The trapping of the impurities can occur for inert ions such as Ar^+ if its energy is high enough to be implanted into the film as in ion implantation. For active ions such as $O_2{}^+$, adsorption is the typical mode of impurity trapping. For such ions, the fraction, f_i, of species i trapped in a film being deposited at the rate of r_d is given by

$$f_i = \frac{(r_a)_i}{(r_a)_i + r_d} \tag{9.17}$$

where $(r_a)_i$ is the rate of adsorption of species i.

The effect of target temperature on the rate of sputtering is minimal unless the target becomes too hot since only physical change is involved. The same can be said for the substrate temperature, since the only thermal effect is through evaporation of the deposited material. The pressure effect is on the transport of sputtered atoms, which is considered in the next chapter.

9.5 PLASMA DEPOSITION AND GAS-SOLID REACTION

Physical sputtering is a major method by which metallization is carried out. However, the fact that any reactive species can be generated in a plasma by simply introducing the desired gases to the electrode system has been exploited by others for film deposition other than metallization. If a film source gas is

TABLE 9.1
Comparisons between sputtering and plasma deposition (Catherine, 1985)

	Sputtering	Plasma
Source	Solid (gas)	Gas
Pressure, torr	$<10^{-2}$	$0.1 \sim 2$
Deposition temperature, °C	~ 25	<300
Deposition rate, nm/min	$0.1 \sim 10$	$1 \sim 50$
Crystallinity	Mostly amorphous (crystalline)	Mostly amorphous (polycrystalline)
DC bias, V	$500 \sim 3000$	<300
Power density, W/cm²	0.5	0.5

introduced to an electrode system, the reactive species generated can lead to deposition at a lower temperature, because of its more reactive nature. Creation of a more active substrate surface by the impact of colliding ions is another enhancement factor in plasma deposition. This type of deposition is often referred to as plasma-assisted or plasma-enhanced deposition, or sometimes plasma-enhanced chemical vapor deposition. The difference between deposition by physical sputtering and plasma deposition may be described in terms of the source. The target material is the source in the case of physical sputtering, but the gas is the source for plasma deposition. Another major difference is that the substrate is usually immersed in the plasma in the case of plasma deposition. In this way, reactive atoms or molecules are more readily accessible to the substrate. Therefore, electrodes may not be present in some cases. An example is the glow generated by induction (rf) heating. Comparisons between sputtering and plasma deposition are given in Table 9.1.

When the substrate is immersed in a plasma, sheaths again form around it. Since the surroundings outside the sheaths is at the plasma potential V_p, and the substrate is at a "floating" potential V_f, which is lower than V_p to repel electrons, the energy barrier the electrons have to overcome is the difference, $(V_p - V_f)$. This floating potential is also shown in Fig. 9-10. Further, the net current to the substrate is zero, i.e., the ion current is the same as the electron current, because of the neutrality of plasma. This potential difference is approximately given (Chen, 1974) by

$$V_p - V_f = \frac{k_B T_e}{2q} \ln\left(\frac{M_i}{2.3m_e}\right) \tag{9.18}$$

where T_e is the electron temperature and m_e is the mass of an electron. This potential difference is sufficiently small for the sputtering to be negligible, which is another reason for immersing the substrate in the plasma.

Example 9.7. The floating potential and electron temperature are determined experimentally by inserting a probe into the plasma. The electrical characteristics of a plasma with a probe (or equivalently immersed substrate) are completely defined by the Langmuir theory (Langmuir, 1923; Langmuir and Mott-Smith, 1924).

However, experimental realization is quite another matter (e.g., Morgan, 1985). Based on the following typical values given by Chapman (1980), calculate the potential drop across the plasma substrate sheath:

$$M_i = 6.6 \times 10^{-23}\ \text{g} \qquad m_e = 9.1 \times 10^{-28}\ \text{g}$$

$$T_e = 23{,}200\ \text{K} \qquad T_i\ (\text{gas temperature}) = 290\ \text{K}$$

It is useful to know that 1 eV corresponds to 11,600 K, which follows from the k_B value ($k_B = 8.62 \times 10^{-5}$ eV/K).

Solution. From Eq. (9.18),

$$V_p - V_f = \frac{k_B T_e}{2q} \ln \frac{6.6 \times 10^{-23}}{2.3 \times 9.1 \times 10^{-28}}$$

$$= \frac{8.62 \times 10^{-5} \times 23{,}200\ (\text{eV})}{2q}\ 10.358$$

$$= \frac{10.36}{q}\ \text{eV}$$

$$= 10.36\ \text{volts}$$

The unique features of plasma deposition are the generation of various reactive species at almost room temperature by colliding hot electrons in the plasma and the creation of energetically favorable substrate surface sites by colliding ions with the substrate surface. These unique features, which are the very reasons for employing the technique, are at the source of extraordinarily complex phenomena that have yet to be unraveled. For deposition kinetics, one needs an understanding of the reactions leading to the formation of reactive species in the plasma. The eventual adspecies are determined by the compatibility of the reactive species in the plasma with the energetics of the substrate surface. Therefore, a full description of the deposition kinetics requires not only the surface state as modified by colliding ions but also the heterogeneous reactions on the substrate. However, because of the complexity, such an understanding is not available for any plasma deposition process.

All ions (radicals) and neutrals in the plasma are originally generated by the impact of colliding electrons with molecules. When the electron impact leads to the formation of neutrals, the process is often referred to as dissociation (decomposition). Examples are:

$$e + H_2 \longrightarrow H + H + e$$

$$e + SiH_4 \longrightarrow SiH_2 + H_2 + e$$

$$e + CF_4 \longrightarrow CF_3 + F + e$$

As the examples show, dissociation leads to reactive neutrals, free radicals, such as H, SiH_2, F and CF_3 but it also leads to stable ("unreactive") neutrals such as

H_2. Ionization by electron impact can take several paths. Examples are:

$$e + Ar \longrightarrow Ar^+ + 2e$$

$$e + SiH_4 \longrightarrow SiH_3^+ + H + 2e$$

$$e + CF_4 \longrightarrow CF_3^- + F$$

The first reaction is simple ionization. The second is dissociative ionization, and the third is dissociative attachment, since the electron combines with CF_3 upon impact. These ions and neutrals can also form various products by reacting among themselves and with other species. Since radical-initiated reactions can lead to many products through propagation, recombination and disproportionation, it is not difficult to envisage a myriad of species present in plasma. Each reaction in the examples can be treated as an elementary reaction. For the reaction, $e + SiH_4 \rightarrow SiH_2 + H_2 + e$, for instance, one can write:

$$r_{SiH_2} = k n_e n_{SiH_4} \tag{9.19}$$

where k is the rate constant, n_e is the electron density, and n_{SiH_4} is the silane density (typically in units of molecules/cm^3 or simply cm^{-3}).

For typical rf discharge systems, electron (and thus positive ion) densities in plasma are between 10^8 and 10^{12} cm^{-3}. Average electron energies are several electron volts while ion (and neutral) energies are at least two orders of magnitude lower. Further, the density of neutrals is greater than that of ions by three orders of magnitude and thus the neutral species are the primary contributors to film deposition (Hess, 1986). Because of the positive, i.e., $(V_p - V_f)$, sheath potential around the substrate, mostly positive ions and electrons but few negative ions reach the substrate, negative ions being much less mobile than electrons. Further, neutrals reach the substrate by diffusion across the sheath, and positive ions arriving at the substrate become immediately neutralized by electrons (Greene and Barnett, 1982). Thus, neutrals are the main adspecies precursors. A determination of the dominant reactive neutrals can be made on the basis of the dissociation energy required for their formation. The reactive neutrals can then become candidates for adsorption precursors.

Example 9.8. According to Turban (1984), the dissociation energies of silane are as follows:

		Dissociation energy, eV
$e + SiH_4 \longrightarrow$	$SiH_3 + H + e$	4.04
	$SiH_2 + H_2 + e$	2.16
	$SiH_2 + 2H + e$	6.7
	$SiH + H + H_2 + e$	5.7
	$Si + 4H + e$	13.2

Determine the ratio of the density of SiH_3 to that of SiH_2 in plasma, assuming Boltzmann statistics. Assume a plasma temperature of 300 K.

Solution. According to Boltzmann statistics, the probability of a molecule overcoming a dissociation energy barrier, E_{da}, and forming products is given by

$\exp(-E_{da}/k_B T)$. Thus, the ratio of SiH_3 density to SiH_2 density, n_{SiH_3} to n_{SiH_2}, is given by

$$\frac{n_{SiH_3}}{n_{SiH_2}} = \frac{\exp(-4.04/k_B T)}{\exp(-2.16/k_B T) + \exp(-6.7/k_B T)}$$

$$= \frac{1}{\exp[(4.04 - 2.16)/k_B T] + \exp[(4.04 - 6.7)/k_B T]}$$

$$= \frac{1}{\exp[1.88/(8.6 \times 10^{-5} \times 300)] + \exp[-2.66/(8.6 \times 10^{-5} \times 300)]}$$

$$= \frac{1}{\exp(72.7) + \exp(-102.9)}$$

$$= \exp(-72.7) = 2.67 \times 10^{-32}$$

An assumption here is that SiH_3 and SiH_2 are formed from SiH_4 only. Note that $k_B = 8.62 \times 10^{-5}$ eV/K (1 eV/molecule = 23.04 kcal/mol). It is seen that the SiH_3 density is negligible compared with n_{SiH_2}. Thus, the reactive neutral with the lowest dissociation energy dominates, particularly at room temperature, since a slight difference in the dissociation energy makes a large difference in the relative density at that temperature.

Deposition rate kinetics can be derived on the basis of assumed adspecies precursors, just as was done in Chap. 5. Although plasma deposition is mostly used on amorphous materials, crystalline structures can also be obtained. As in any type of deposition, the key to the crystallinity is the relative rate of precursor adsorption with respect to that of surface migration of adspecies. Either a polycrystalline or an amorphous material will result if the adsorption rate is higher than the migration rate. In plasma deposition, these rates are determined by the substrate temperature and the flux to the substrate of the adspecies precursor. Monocrystalline films occur at high substrate temperatures. For instance, an epitaxial silicon film has been grown by plasma deposition by heating the substrate to 750°C (Donahue *et al.*, 1984). As discussed in detail in Sec. 5.4, first-order kinetics results when an amorphous film is formed by crosslinking:

$$r_a = KC_a = J_a \tag{9.20}$$

where r_a is the rate of amorphous film deposition per unit surface area, C_a is the adspecies concentration on the substrate surface, and J_a is the flux of an adspecies precursor, which is usually one of the reactive neutrals diffusing through the sheath around the substrate. If some level of crystallinity is present in the amorphous film, the rate is given (Sec. 5.4) by

$$r_a = \frac{k'C_a}{1 + KC_a} \tag{9.21}$$

The procedures of Sec. 5.4 can be applied to the kinetics of poly- and monocrystalline film growth. Any substrate surface modification made by colliding ions that promotes deposition would appear in the form of larger rate constants when compared with the film grown by conventional CVD.

Silicon nitride in the form of Si_xN_{1-x} is often grown as a passivating layer by plasma deposition. The reactants are usually either SiH_4/N_2 or SiH_4/NH_3 and the film is grown at temperatures below 300°C (e.g., Gorowitz *et al.*, 1985). Silicides used as contact materials are also often grown by plasma deposition. For tungsten silicide, for instance, the reactants are WF_6 and SiH_4 (e.g., Akimoto and Wantanabe, 1981). For the deposition involving two species, one may consider competitive adsorption followed by incorporation into the solid structure. For the competitive adsorption, one may write:

$$A(g) + S \underset{}{\overset{K_A}{\rightleftharpoons}} A \cdot S$$

$$B(g) + S \underset{}{\overset{K_B}{\rightleftharpoons}} B \cdot S$$

where A and B are the adspecies precursors for the film atom ratio in the form of A_xB_{1-x}, and A·S and B·S are the corresponding adspecies. It follows (Sec. 5.4) from the adsorption steps that

$$\frac{C_{A\cdot S}}{C_t} = \frac{K_A C_A}{1 + K_A C_A + K_B C_B} \tag{9.22}$$

$$\frac{C_{B\cdot S}}{C_t} = \frac{K_B C_B}{1 + K_A C_A + K_B C_B} \tag{9.23}$$

where K_A and K_B are the adsorption equilibrium constants, and C_A and C_B are the concentrations of the precursors A and B. Each adspecies can become part of the amorphous structure independently. They can also combine into the film structure. Therefore, the steps for incorporation into the amorphous structure are

$$\begin{aligned} \alpha A \cdot S &\xrightarrow{k_A} A_\alpha(a) \\ \beta B \cdot S &\xrightarrow{k_B} B_\beta(a) \\ A \cdot S + \mu B \cdot S &\xrightarrow{k_c} AB_\mu(a) \end{aligned} \tag{9.24}$$

where $A_\alpha(a)$ and $B_\beta(a)$, respectively, are α number of adspecies A and β number of adspecies B incorporated into the amorphous structure, and $AB_\mu(a)$ is the part of amorphous incorporation involving one adspecies A and μ number of adspecies B. It follows from Eqs. (9.22), (9.23), and (9.24) that the atom ratio x is given by

$$x = \frac{\alpha r_A + r_c/\mu}{\alpha r_A + \beta r_B + r_c} \tag{9.25}$$

where r_A, r_B, and r_c are given by

$$r_A = \left(\frac{k_A K_A C_A}{1 + K_A C_A + K_B C_B}\right)^\alpha \tag{9.26}$$

$$r_B = \left(\frac{k_B K_B C_B}{1 + K_A C_A + K_B C_B}\right)^\beta \tag{9.27}$$

$$r_c = \frac{k_c K_A K_B^\mu C_A C_B^\mu}{(1 + K_A C_A + K_B C_B)^{1+\mu}} \tag{9.28}$$

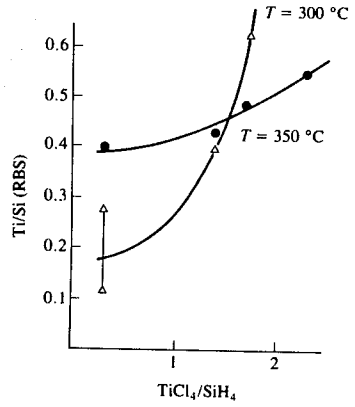

FIGURE 9-11
Film composition as a function of gas phase composition for plasma-enhanced CVD (Kemper *et al.*, 1985).

Example 9.9. Experimental results obtained by Kemper *et al.* (1985) are shown in Fig. 9-11 for Ti_xSi_{1-x} silicide film prepared by plasma deposition. The results show the Ti/Si atom ratio as a function of gas phase composition, $TiCl_4/SiH_4$. The concentration in Eqs. (9.25) through (9.28) are those at the substrate, whereas the concentration ratio in Fig. 9-11 is for the bulk gas phase. Therefore, the concentration ratio cannot be used in the equations directly. For the sake of illustration, assume the concentration ratio to be the adspecies concentration ratio at the surface. Reduce Eq. (9.25) for the following cases:

(*a*) r_c is negligible.
(*b*) r_c is negligible and $\alpha = \beta$.
(*c*) $\alpha = \beta = 2$, $\mu = 1$.

Compare the reduced results with the data in Fig. 9-11.

Solution
(*a*) If r_c is negligible, Eq. (9.25) reduces to

$$x = \frac{\alpha r_A}{\alpha r_A + \beta r_B} \tag{A}$$

$$= \frac{1}{1 + (\beta/\alpha)\{(k_B K_B C_B)^\beta / [(1 + K_A C_A + K_B C_B)^{\beta-\alpha}(k_A K_A C_A)^\alpha]\}}$$

(*b*) If $\alpha = \beta$, one has, from Eq. (A),

$$x = \frac{1}{1 + k_B K_B C_B/(k_A K_A C_A)} \tag{B}$$

(*c*) If $\alpha = \beta = 2$ and $\mu = 1$, it follows from Eqs. (9.26) through (9.28) that

$$x = \frac{2(k_A K_A C_A)^2 + k_c K_A K_A C_A C_B/\mu}{2(k_A K_A C_A)^2 + 2(k_A K_B C_B)^2 + k_c K_A K_B C_A C_B} \tag{C}$$

Under the assumption, $TiCl_4/SiH_4$ is equal to C_A/C_B. In terms of the atom ratio Ti/Si, x can be expressed as

$$x = \frac{\text{Ti/Si}}{1 + \text{Ti/Si}} \tag{D}$$

It can be deduced from Eqs. (B) and (D) that the data cannot be represented by Eq. (B). Additional information would be necessary for the other cases.

It should be recognized that the kinetics for plasma-enhanced CVD (PECVD) are in the same form as for the conventional CVD counterpart. The only difference is in the activation energy. Because of enhancement from the surface modification by colliding ions, the activation energy for PECVD is generally lower than that for conventional CVD and depends on the ion energy.

While plasma deposition can perhaps be traced to the work of Alt *et al.* (1963) for semiconductor processing, the advantage of low-temperature processing permitted by plasma was also recognized for the oxidation of native silicon (Ligenza, 1965). Reactions of gaseous species from a plasma with a native substrate, as in oxidation or nitridation of silicon, can be categorized as plasma gas-solid reactions. As in plasma deposition, reactive species generated in the plasma are utilized for the gas-solid reaction. The substrate can be immersed in a plasma or it can be placed outside. When the substrate is placed outside the plasma on an anode, the process is referred to as anodization, although it is usually limited to oxidation reactions.

The rate of oxidation or nitridation by plasma gas-solid reactions can be expressed in exactly the same manner as for conventional (thermal) gas-solid reactions (Sec. 5.5). Although the formulation is the same, some specifics are different. For one, it is much more difficult to identify which reactive species are primarily responsible for the plasma gas-solid reaction. For another, the transport mechanism from the bulk gas to the substrate surface is different. For thermal gas-solid reactions, film transport is by molecular diffusion. For plasma gas-solid reactions, transport across the sheath is by molecular diffusion for neutral species but can be dominated by drift for negative ions when the substrate is placed on an anode. In both cases, the distance of diffusion or drift, which is the sheath thickness, is dictated by the applied potential.

The reactive species generated in oxygen plasmas are

$$O_2 + e \longrightarrow O_2^+ + 2e$$
$$O_2 + e \longrightarrow 2O + e$$
$$O + e \longrightarrow O^-$$
$$O_2^+ + e \longrightarrow 2O$$

Although the reactive species resulting from electron collisions are O_2^+, O, and O^-, there is uncertainty as to which is the dominant reactive species (Friedel and Gourrier, 1983; Barlow *et al.*, 1985). However, certain inferences can be made on the basis of the type of discharge. Plasma anodization, which is by far the most commonly used method, involves placing the substrate on an anode. A negatively

charged sheath forms around the anode due to the dc discharge. Therefore, negative ions can easily drift to the substrate whereas positive ions cannot because of an energy barrier. Thus, the dominant reactive species in this case are likely to be O and O^-. In the case of rf discharges, the transport of reactive species across the sheath is exactly the same as in plasma deposition. Thus, the dominant reactive species would be neutral, i.e., O.

The rate of oxidation as affected by transport processes can be derived in exactly the same manner as for thermal oxidation (Sec. 5.5). If neutral atomic oxygen is the dominant species during oxidation, the rate of oxidation is given by Eq. (5.89) with k_m replaced by D_o/d and C_b replaced by N_o. Here D_o is the molecular diffusivity of atomic oxygen, d is the sheath thickness, and N_o is the atomic oxygen concentration in the oxygen plasma. While the sheath thickness in rf discharges is determined by the applied voltage, the thickness in dc discharge can be varied for any voltage (Sec. 9.3) by simply moving the anode toward the plasma.

Example 9.10. Both neutral and negative oxygen ions can be the dominant species for plasma oxidation in dc discharges. However, assume for this example that the negative ion is primarily responsible for the oxidation. Because of the negative discharge, not only diffusion but also drift contributes to the flux of the ion to the substrate. For this case, one can write:

$$\mu_i n_i E + D_i \frac{dn_i}{dx} = 0 \tag{A}$$

for the density of the negative ion n_i in the negative sheath. Here μ_i and D_i are the mobility and diffusivity, respectively, of the ion, E is the electric field, and x is the distance normal to the substrate surface. Noting that $n_i = (n_i)_0$ at $x = 0$ and $-E = dV/dx$ where V is the potential, the solution of Eq. (A) yields

$$n_i(x) = (n_i)_0 \exp\left[\frac{q}{kT}(\Delta V)_x\right] \tag{B}$$

where $(\Delta V)_x$ is the voltage drop across a distance x and the Einstein relationship $(D/\mu = kT/q)$ has been used. At the surface of the substrate, $x = d$ and $n_i = (n_i)_s$. Thus,

$$(n_i)_s = (n_i)_0 \exp\left(\frac{q\,\Delta V}{kT}\right) = (n_i)_0 v_i \tag{C}$$

where ΔV is now the voltage drop across the sheath. Using the approach in Sec. 5.5 and Eq. (C), derive a rate expression for the oxidation.

Solution. Rewriting Eq. (C) in terms of concentration, one has

$$N_s = N_p v_i \tag{D}$$

where N_s is $(n_i)_s$ and N_p is $(n_i)_0$ in terms of molar concentration. Equation (5.82) (Sec. 5.5) can be written as

$$-D_s \frac{dN}{dx} = D_s\left(\frac{N_s - N_i}{l}\right) \tag{E}$$

where N_i is the concentration at the oxide-solid reactant interface, D_s is the ion diffusivity in the oxide, and l is the sheath thickness. The equation corresponding to Eq. (5.83) is

$$r_c = k_i N_i \tag{F}$$

where k_i is the rate constant for the reaction by the ion. One then has, from Eqs. (D), (E), and (F) with the aid of Eqs. (5.86) and (5.87),

$$m\rho'_M \frac{dl}{dt} = \frac{k_i N_p v_i}{1 + k_i l/D_s} \tag{G}$$

which corresponds to Eq. (5.88). Therefore, the rate of oxidation is given by

$$\begin{aligned} l^2 + A_i l &= B_i t \\ A_i &= 2D_s/k_i \\ B_i &= \frac{2D_s v_i N_p}{m\rho'_M} \end{aligned} \tag{H}$$

Note that N_p is the negative ion concentration in the plasma.

When both neutral oxygen atoms and their negative ions are contributing to the oxidation, the overall oxidation rate can be written as

$$r_o = r_i + r_n$$

Furthermore, one can write, in place of Eq. (5.86),

$$\left(\frac{m}{A_i}\right)\frac{dN_m}{dt} = r_o = r_i + r_n \tag{9.29}$$

where r_i is the rate due to the ion and r_n is that for the neutral. A rate expression that is not in the form of Eq. (5.89) (Deal-Grove type of model) results (see Prob. 9.10).

Plasma nitridation (e.g., Petro *et al.*, 1986) is essentially the same as plasma oxidation in the framework of gas-solid reactions. Therefore, the rate expression derived for oxidation also applies to nitridation.

9.6 PLASMA ETCHING

The unique feature of plasma etching as compared to physical sputtering lies in the gasification of substrate at the surface by the reactive species generated in plasma. The modification of substrate surface by bombarding ions which significantly increases the rate of gas-solid reaction (gasification) is more important than the nature of the reactive species. This effect is clearly shown in Fig. 9-12. When only XeF_2 gas is used, the etch rate can be attributed mainly to the gasification of silicon by silicon fluoride whereas it is due to physical sputtering when only argon ions are used. When both are used, the etch rate becomes much greater than the sum of the individual rates, as evident from the figure. While the exact mechanism may be subject to dispute, there is no doubt that the modifi-

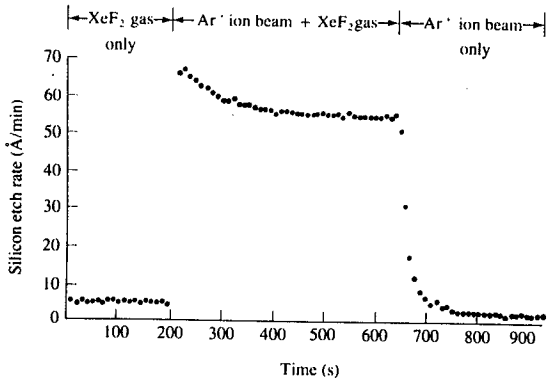

FIGURE 9-12
Effect of ion bombardment on etching (Coburn and Winters, 1979).

cation of the surface and/or surface species by bombarding ions is responsible for the synergistic effect. Although plasma was not involved in the etching, the results in the figure clearly show the role of ions.

Ions in plasma approach perpendicularly to the substrate surface under the usual operating conditions because of the directed electric field. The normal incidence is assured when the sheath thickness is much larger than the vertical dimension of window openings and the mean free path is larger than the sheath thickness. Ordinarily, therefore, anisotropy is easier to achieve than with wet etching. In this regard, two types of plasma etching are of interest. Plasma etching is ion-induced if no etching takes place in the absence of ions. In this case, anisotropy is normally expected since there cannot be any lateral etching with the normally incident ions. Plasma etching is ion-enhanced if etching can take place in the absence of ions, but it is greatly enhanced by ion bombardment. However, for ion-enhanced etching, the window to be etched out can be undercut. In either case, the physical momentum transfer from colliding ions is the initiator for plasma etching.

In plasma etching, the reactive neutral species in general are responsible for actual etching. The role of ions is to make the substrate surface more active with respect to the reactive neutral species and at the same time to provide the directionality of the etched surface. Typical gases used are halogen compounds such as CF_4 and Cl_2. Additional gases are also added such as H_2 or O_2 to provide desired selectivity and edge profile (Flamm and Donnelly, 1981). The dominant ion in CF_4 plasma is CF_3^+ (Harper *et al.*, 1981), which is primarily produced by the following:

$$e + CF_4 \longrightarrow CF_3^+ + F + 2e$$

The atomic fluorine can be produced by a number of other reactions. In chlorine plasma, the dominant ion is believed to be Cl_2^+. The reactive chlorine atom can be generated by

$$e + Cl_2 \longrightarrow 2Cl + e$$

The kinetics of plasma etching can be treated in the general framework of gasification taking place on the substrate surface. The neutral species formed in the plasma adsorbs on the substrate surface upon diffusing through the plasma sheath. The adsorbed species then goes through surface reaction(s) which lead to surface species that are precursors to the gasified species. The surface species then desorbs, resulting in the gasification of the substrate. As with any heterogeneous reaction sequence, one of these three steps can be rate-limiting. It has been found in plasma etching of InP in chlorine plasma, for instance, that the activation energy of the etching is close to the sublimation energy of $InCP_3$ (Donnelly *et al.*, 1982). This indicates that the rate-limiting step could be the desorption step.

The selectivity of an etchant with respect to two different materials is an important factor in pattern delineation. An example would be the selectivity of an etchant with respect to the silicon oxide layer and the underlying silicon. In opening a window through the oxide layer, an ideal situation is one in which the etchant etches the oxide but not the silicon. It is known in CF_4 plasma etching that addition of H_2 does not greatly affect the etch rate of SiO_2 but the Si etch rate decreases with increasing H_2 content (Eprath, 1979). This has to do with the number of fluorine atoms available for etching. In the plasma, hydrogen atoms can readily combine with fluorine atoms to form HF. The same process also takes place in the sheath. Therefore, the etch rate of silicon decreases with increasing H_2 content. When silicon dioxide is exposed to the plasma, oxygen liberated from the oxide surface competes with the fluorine atom for combination with hydrogen. Therefore, the etch rate of silicon oxide decreases slightly with increasing H_2 content. The effect of adding O_2 to CF_4 plasma, shown in Fig. 9-13, also has to do with the availability of fluorine atoms. One major source of disappearance of fluorine atoms is recombination with CF_x ions. As the oxygen concentration increases, oxygen combines with CF_x ions to produce species such as COF_2, CO, etc., thereby decreasing the availability of CF_x ions, resulting in increased fluorine atom levels in the plasma. When the oxygen concentration becomes too high, dilution of the plasma by oxygen dominates over enhancement and a maximum appears in the etch rate. If plasma reactions were solely responsible for the behavior in Fig. 9-13, similar trends would be observed for both Si and SiO_2. The observed difference has been attributed to the chemisorption behavior of oxygen on the substrates (Mogab *et al.*, 1978). On Si, oxygen chemisorbs whereas chemisorption on SiO_2 should be negligible. Inhibition by chemisorption of oxygen has been proposed as the reason for the more rapid decrease in the etch rate of Si at higher oxygen contents compared with the etch rate decrease of SiO_2.

When a halogen compound containing carbon is used, there is invariably carbon deposited on the substrate surface. This is caused by impact dissociation

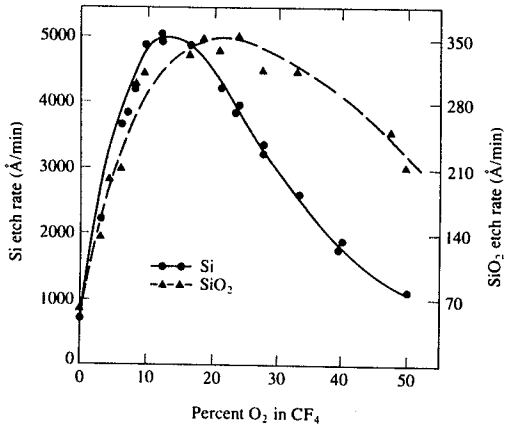

FIGURE 9-13
Etching selectivity as affected by oxygen addition (Mogab *et al.*, 1978).

of the ions on the surface. The carbon deposit has to be sputtered away, if the surface is to be etched. On the other hand, the deposit can be used as a means of achieving etching selectivity. Another problem is the formation of polymer both in the plasma and on the substrate surface in the form of $(CF_2)_n$, for example, when the ion concentration is relatively high. Here, again, the polymer formed can be used as a protective coating.

The etching kinetics for both ion-induced and ion-enhanced plasma etching can be treated in the same way. If one lets r_o be the observed intrinsic rate of etching and r_u the rate in the absence of ions, then the rate of etching r for both cases can be expressed as

$$r = r_o - r_u \tag{9.30}$$

For ion-induced etching, $r_u = 0$ and thus $r = r_o$. For ion-enhanced etching, r represents the rate enhancement due to the modification of surface and/or surface species by colliding ions. In general, adsorption processes of neutral species may involve successive adsorption steps (Flamm and Donnelly, 1981):

$$\begin{aligned} A + S &\rightleftharpoons A\cdot S \\ A\cdot S + A &\rightleftharpoons (2A)\cdot S \\ [(x-1)A]\cdot S + A &\rightleftharpoons (xA)\cdot S \\ (xA)\cdot S + A &\rightleftharpoons [(x+1)A]\cdot S \end{aligned}$$

where A is the active neutral species. $A\cdot S$ is the substrate surface atom S with one adsorbed species and $(2A)\cdot S$ is the same but with two adsorbed neutral

species, etc. Depending on the energetics of the surface sites, some of the adsorbed species may react to form product precursors in the adsorbed state by electron reconfiguration:

$$\begin{aligned} (2A)\cdot S &\rightleftharpoons A_2S\cdot S \\ &\vdots \\ (xA)\cdot S &\rightleftharpoons A_xS\cdot S \end{aligned}$$

where $A_xS\cdot S$ is the product precursor with x number of neutral species bonded to the underlying substrate surface atom S. Finally, the product precursors desorb, yielding the gasified product A_xS:

$$\begin{aligned} A_2S\cdot S &\rightleftharpoons A_2S(g) \\ &\vdots \\ A_xS\cdot S &\rightleftharpoons A_xS(g) \end{aligned}$$

Although rate expressions encompassing all the steps involved can be written, they are too complex and cumbersome to use. As discussed in Chap. 5, it is often sufficient to consider only the dominant surface species for the purpose of describing the kinetics. As an example, consider etching of silicon in CF_4 plasma. The main products of etching are SiF_2 and SiF_4. One may assume the dominant surface species to be the adsorbed SiF_2, as proposed by Donnelly and Flamm (1980), or in the above notation, $(2A)\cdot S$, where S is for surface Si atom and A symbolizes fluorine. Then, the surface reaction steps can be written as follows:

$$\begin{aligned} A(g) + S &\overset{K_1}{\rightleftharpoons} A\cdot S & (F + S &\rightleftharpoons F\cdot S) \\ A\cdot S + A(g) &\overset{K_2}{\rightleftharpoons} (2A)\cdot S & [F\cdot S + F &\rightleftharpoons (2F)\cdot S] \\ (2A)\cdot S &\rightleftharpoons A_2S\cdot S & [(2F)\cdot S &\rightleftharpoons F_2S\cdot S] \\ A_2S\cdot S &\overset{K_d}{\rightleftharpoons} A_2S(g) + S & [F_2S\cdot S &\rightleftharpoons SiF_2(g) + S] \end{aligned}$$

Further, one of the steps may be assumed to be the rate-controlling step. Suppose that the third step is the controlling step, for which one can write

$$(2A)\cdot S \xrightarrow{k_s} A_2S\cdot S$$

Note that this reaction represents the formation of the precursor for the gasified product A_2S in the form attached to the underlying silicon atom. Thus, $A_2S\cdot S$ is a notation for the state and does not involve any additional vacant site exposed to the gaseous environment. This fact is reflected in the surface reaction written above. Following the procedures detailed in Chap. 5, one has

$$\frac{C_v}{C_t} = \frac{1}{1 + K_1(C_A + K_2 C_A) + K_d C_{A_2S}} \tag{9.31}$$

and

$$r = k_s C_{2A\cdot S} = k_s K_1 K_2 C_v C_A^2 \tag{9.32}$$

where C_t is the surface concentration of total silicon atom sites and C_v is that of vacant silicon sites. Use of Eq. (9.31) in Eq. (9.32) yields

$$r = \frac{kC_A^2}{1 + K_1(C_A + K_2 C_A) + K_d C_{A_2S}} \tag{9.33}$$

In terms of the species F and SiF_2, the rate can be rewritten as

$$r = \frac{kC_F^2}{1 + K_1(C_F + K_2 C_F) + K_d C_{SiF_2}} \tag{9.34}$$

where C_F is the concentration of the neutral fluorine atom at the silicon surface and C_{SiF_2} is the surface concentration of SiF_2.

It is noted in this regard that the activation energies of the rate constants in Eq. (9.34) cannot be the same, even for the same plasma conditions, if the ion energy changes. This is due to the fact that surface modification and the resulting surface energetics are determined by the momentum of the colliding ions with the substrate surface. Thus, the activation energies depend on the ion energy.

The kinetics of plasma etching invariably involve terms for the neutral species concentration at the substrate surface. To relate this to feed conditions, the concentrations of the species in the plasma have to be known, which in turn has to be related to the surface concentration. Transport phenomena are the link to these relationships, which is treated in the next chapter.

NOTATION

A	Solid surface area (L^2)
A_i	Cross-sectional surface area (L^2)
C_a	Surface concentration of adspecies (mol/L^2)
C_A, C_B	Concentrations of species A and B, respectively (mol/L^3)
$C_{A\cdot S}$, $C_{B\cdot S}$	Concentrations of surface species A·S and B·S, respectively (mol/L^2)
C_v	Surface concentration of vacant sites (sites/L^2)
C_t	Surface concentration of total available sites (sites/L^2)
d	Sheath thickness (L)
D_i	Ion diffusivity (L^2/t)
E	Ion energy (E); electric field (V/L)
E_{th}	Threshold energy (E)
f_i	Fraction of species i trapped in film
G	Linear growth rate (L/T)
j_e	Cathode ion current density (I/L^2t)
j_i	Ion current density (I/L^2t)
J_a	Flux of adspecies (mol/L^2t)
k	Rate constant (units dependent on concentration units)
k_B	Boltzmann constant

K, K_A, K_B	Equilibrium constants (units dependent on concentration units)
L	Distance from center of substrate plane (L)
m	Mass of molecule (M)
m_e	Mass of electron (M)
M	Molecular weight (M/mol)
M_i	Ion mass (M)
M_s	Solid molecular weight (M/mol)
n_e	Electron density (electron/L^3)
n_i	Ion density (ions/L^3)
N	Number of molecules
N_A	Avogadro's number
N_m	Moles of species m
p	Partial pressure
p^*	Saturation pressure (P)
q	Electron charge (C)
r	Distance between source and substrate (L); rate of reaction (mol/L^2t)
r_c	Rate of condensation (atom/L^2t)
r_D	Rate of deposition (M/L^2t)
$(r_D)_0$	r_D directly above and r away from source
r_i	Rate due to ion (mol/L^2t)
r_n	Rate due to neutral (mol/L^2t)
r_s	Rate of sputtering (atom/L^2t)
S	Sputtering yield (atom/ion)
t	Time
T	Temperature
T_e	Electron temperature (T)
U	Surface binding energy (E)
V	Mass rate of evaporation (M/L^2t)
V_a	Applied voltage (V)
V_{dc}	dc bias in asymmetrical, capacitive rf plasma (V)
V_f	Floating potential (V)
V_p	Plasma potential (V)
V_{sp}	Sheath potential (V)
V_t	Mass rate of evaporation (M/t)
x	Spatial coordinate (L); atom fraction in binary alloy
Z_t	Atomic number of target material
Z_x	Atomic number of gas species

Greek letters

α	Constant; quantity defined in Eq. (9.11); angle in Fig. 9-1
β	Constant
μ	Constant; number of secondary electrons ejected per incident ion
μ_i	Ion mobility (L^2/Vt)

ρ_s	Solid density (M/L^3)
ω	Angle in Fig. 9-1
Ω	Angle in Fig. 9-1

Units

C	Coulomb
E	Energy
I	Current
L	Length
M	Mass
P	Pressure (M/Lt^2)
t	Time
T	Temperature
V	Voltage

PROBLEMS

9.1. Plot the relative rate, $r_D/(r_D)_0$, as a function of L/r for both point and small area evaporant sources up to L/r of 2. Comment on the uniformity of a film deposited onto a flat substrate for the two cases.

9.2. Suppose metallization is carried out for a metal strip 1 μm wide that is defined by a resist 1.5 μm thick. For the evaporation from a point source for metallization, which is 5 cm away from the center of the resist window, determine the maximum length of the groove that can be filled with a maximum thickness deviation less than 1 percent. For the maximum deposition rate of 1×10^{-5} g/(cm^2·s), calculate the time required to fill the resist window. Assume the metal density to be 4 g/cm^3.

9.3. For gold metallization at 300 K, suppose that the main residual gas is oxygen which constitutes 1 percent of the volume. Calculate the fraction of oxygen incorporated into the metal deposit. Use Fig. 9-3. The desired linear deposition rate is 1 nm/s.

9.4. For MBE, which is an epitaxial process, the rate of growth is dictated by the rate of surface migration of adatoms; i.e., the net rate of condensation should be less than the rate of surface migration. Otherwise, a monocrystalline structure cannot be obtained. The surface migration rate decreases exponentially with decreasing temperature. Suppose that the migration rate corresponds to 0.1 nm/min at 700 °C. Calculate the MBE chamber pressure required for Si MBE at 700 °C.

9.5. A dc discharge is used for tantalum deposition. The measured cathode voltage and current, respectively, are 700 volts and 4 mA in an argon environment. The cathode (target) area is 20 cm^2. Calculate the rate of sputtering, assuming that the contribution to the current by secondary electrons is 10 percent. The distribution of sputtered material deposited on the substrate surface also follows the cosine law but is dependent on the ratio of target diameter to electrode separation. When this ratio is larger than, say, 25, the rate of deposition is essentially the same as the rate of sputtering and the thickness distribution is uniform up to a value of 4 for the ratio of the distance from the center to electrode separation (Maissel, 1970). Determine the ratio of the target diameter to the distance from the center that satisfies the conditions. Discuss whether the electrode separation can be freely chosen.

9.6. Consider aluminum deposition by rf sputtering. For a symmetrical, parallel-plate system, the applied voltage is 120 volts and the electrode area is 20 cm^2. For aluminum, the sputtering yield S is given by

$$S(\text{atom/ion}) = 2.257(E^{1/2} - 0.013^{1/2})$$

Assuming that the root mean square current is 0.08 A, calculate the rate of sputtering.

9.7. Electrons accelerated by an applied field cause activation and formation of ions and reactive species in a plasma by collisions. Consider the following process:

$$e + SiH_4 \longrightarrow SiH_2 + H_2 + e$$

It is known that the activation energy is 2.16 eV. For a SiH_4 plasma at 1 torr, suppose that the ion density is 10^{11} cm^{-3}. Calculate the rate of formation of SiH_2 at 300 K in the plasma by the above process, assuming that the preexponential factor is 10^{24} cm^3/s.

9.8. Polymer deposition on p-type silicon substrates using plasma-enhanced CVD has been reported by Nguyen *et al.* (1985). Their data show that the polymer deposition rate increases exponentially with the power input, holding all other conditions constant. They show that the deposition rate is almost zero below a certain power input. To a first degree of approximation, one may assume the power input to be proportional to the ion energy. The enhancement of the deposition rate can be attributed to the change of the silicon surface by colliding ions, which could reduce the activation energy for the deposition. Based on the premises stated, postulate the dependence of the deposition rate on the ion energy. Assume the rates to be intrinsic. Use the rate in the form, $r_c = kf(C)$.

9.9. The rate of formation of SiH_2 in the plasma considered in Prob. 9.7 is 1.7×10^{15} molecules/(cm^3·s). Suppose the surface area of deposition for polysilicon is 5 cm^2. Determine the maximum constant linear deposition rate (in centimeters per minute) that is sustainable. Discuss what happens if the substrate temperature is high enough that the potential deposition rate is higher than that corresponding to 1.7×10^{15} molecules/(cm^3·s). Assume that the generation of adspecies SiH_2 is by Eq. (9.19) and that the adspecies for the polycrystalline silicon is SiH_2.

9.10. Plasma gas-solid reactions such as plasma oxidation or nitridation are due to both negative ions and neutrals supplied by the plasma. Show for such reactions that the rate of oxidation or nitridation, when both contribute to the reaction, can be determined from Eq. (9.29) written in the following form:

$$m\rho'_M \frac{dl}{dt} = \frac{k_i N_p v_i}{1 + k_i l/D_s} + \frac{kN_n}{1 + kD_0/d + kl/D_{sn}} \qquad \text{(A)}$$

where d is the sheath thickness, k is the rate constant for the neutral, N_n is the neutral concentration in the plasma, D_0 is the gas phase diffusivity of the neutral, and D_{sn} is the diffusivity of the neutral in the solid. Show that Eq. (A) does not lead to the Deal-Grove type of relationship.

9.11. Ion-induced or ion-enhanced etching can be carried out in the absence of plasma. Separate sources of ion and gas species can be used for the etching. In fact, the result shown in Fig. 9-11 was obtained by feeding XeF_2 gas from the gas source directed to the substrate surface while a separate argon ion was directed to the same surface.

Consider the ion-enhanced etching by XeF_2 in the absence of plasma. According to Chuang (1980), XeF_2 adsorbs on silicon surface by dissociation, although the stoichiometry is not clear, and the dominant surface species is SiF_2. Assume the following adsorption/dissociation:

$$XeF_2(g) + S \rightleftharpoons S\cdot F_2 + Xe(g) \qquad \text{(A)}$$

where S is the silicon site. Tu *et al.* (1981) have observed that about 75 percent of Si leaving the surface are in the form of SiF_4. Thus, one may postulate the following steps:

$$S\cdot F_2 + XeF_2(g) \rightleftharpoons S\cdot(SF_4) + Xe(g) \qquad \text{(B)}$$

$$S\cdot(SF_4) \rightleftharpoons SiF_4(g) + S \qquad \text{(C)}$$

Equation (B) represents the surface reaction leading to the formation of the surface species Si-SiF_4 and Eq. (C) represents desorption of the species SiF_4 attached to the underlying Si site, $S\cdot(SF_4)$. Derive the kinetics of etching for each of three cases in which one of the steps is rate-controlling.

9.12. For the etching of Si by XeF_2 with separate sources of ion and the etchant (Fig. P9-12), Gerlach-Meyer (1981) gives etching data for three types of ions as shown in the figure. The flow rate can be taken as equivalent to the concentration of XeF_2. The data have already been reduced such that the etching is solely for the ion-enhanced part, that is, r in Eq. (9.30). It should be clear from the results of Prob. 9.11 that none of the kinetics derived can describe the data, even when one assumes SiF_2 to be the dominating (sole) surface species. With additional information that the

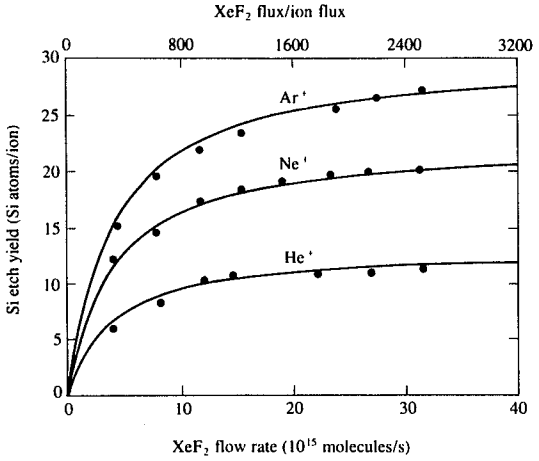

FIGURE P9-12
Etching data of Gerlach-Meyer (1981).

surface coverage by SiF_2 (to be more precise SiF_x) is almost complete and that the ion energy is the same for all ions in the figure, one may postulate the following mechanism:

$$XeF_2(g) + S \rightleftharpoons S\cdot F_2 + Xe(g); \qquad \text{complete coverage by } S\cdot F_2$$

$$S\cdot F_2 \underset{k_r}{\overset{k_i\,(\text{ion})}{\rightleftharpoons}} S\cdot F_2^*$$

$$S\cdot F_2^* + XeF_2(g) \xrightarrow{k^*} SiF_4(g) + Xe(g)$$

The second step is for the activation of the surface species by colliding ions. The rate of etching is then given by

$$r = k^* C_{S\cdot F_2^*} C_A \qquad \text{where } C_A = C_{XeF_2} \qquad \text{(A)}$$

Invoke the pseudo steady-state approximation for the activated surface species $S\cdot F_2^*$ to arrive at the following:

$$r = \frac{k_i C_t k^* C_A}{k_r + k^* C_A} \qquad \text{where } C_{S\cdot F_2} = C_t \qquad \text{(B)}$$

Noting that the only rate constant dependent on the ion type is k_i, offer a postulation for the differences due to the ion type.

REFERENCES

Akimoto, K., and K. Wantanabe: *Appl. Phys. Lett.*, vol. 39, p. 445, 1981.
Alt, L. L., S. W. Ing, and K. W. Laendle: *J. Electrochem. Soc.*, vol. 110, p. 465, 1963.
Barlow, K. J., A. Kiermasz, and W. Eccleston: in G. S. Mathad *et al.* (eds.), *Plasma Processing*, The Electrochemical Society, Pennington, N.J., 1985.
Bollinger, D., and R. Fink: *Solid State Technol.*, vol. 25, p. 79, 1980.
Brown, S. C.: *Introduction to Electrical Discharge in Gases*, McGraw-Hill, New York, 1966.
Catherine, Y.: in G. S. Mathad *et al.* (eds.), *Plasma Processing*, The Electrochemical Society, Pennington, N.J., 1985.
Chapman, B.: *Glow Discharge Processes*, Wiley, New York, 1980.
Chen, F. F.: *Introduction to Plasma Physics*, Plenum Press, New York, 1974.
Cho, A. Y.: *Proceedings of Compound Semiconductor Growth, Processing and Devices for the 1990s*, Japan/US Perspective, Gainesville, Fla., October 1987.
Chuang, T. J.: *J. Appl. Phys.*, vol. 51, p. 2614, 1980.
Coburn, J. W., and E. Kay: *J. Appl. Phys.*, vol. 43, p. 4965, 1972.
——— and H. F. Winters: *J. Appl. Phys.*, vol. 50, p. 3189, 1979.
———, E. Taglaner, and E. Kay: *Jap. J. Appl. Phys.*, suppl. 2, p. 501, 1974.
Donahue, T. J., W. R. Burger, and R. Reif: *Appl. Phys. Lett.*, vol. 44, p. 346, 1984.
Donnelly, V. M., and D. L. Flamm: *J. Appl. Phys.*, vol. 51, p. 5273, 1980.
Eprath, L. M.: *J. Electrochem. Soc.*, vol. 126, p. 1419, 1979.
Erskine, J. C., and A. Cserhati: *J. Vac. Soc. Technol.*, vol. 15, p. 1823, 1978.
Flamm, D. L., and V. M. Donnelly: *Plasma Chem. and Plasma Proc.*, vol. 1, p. 317, 1981.
——— and G. K. Herb: *A Short Course in Plasma Etching*, chap. 1, Academic Press, 1988.
———, V. M. Donnelly, and J. A. Mucha: *J. Appl. Phys.*, vol. 52, p. 3633, 1978.
Friedel, P., and S. Gourier: *J. Phys. Chem. Solids*, vol. 44, p. 353, 1983.
Gerlach-Meyer, U.: *Surface Sci.*, vol. 103, p. 524, 1981.
Glang, R.: in L. Maissel and R. Glang (eds.), *Handbook of Thin Film Technology*, chap. 1, McGraw-Hill, New York, 1970.

Gorowitz, B., T. B. Gorezyea, and R. J. Saia: *Solid State Technol.*, p. 179, June 1985.
Greene, J. E., and S. A. Barnett: *J. Vac. Sci. Technol.*, vol. 21, p. 285, 1982.
Harper, J. M. F., J. J. Cuomo, P. A. Leary, G. M. Summa, H. R. Kaufmann, and F. J. Bresnock: *J. Electrochem. Soc.*, vol. 128, p. 1077, 1981.
Hasted, J. B.: *Physics of Atomic Collision*, Butterworth, London, 1964.
Hess, D. W.: *Ann. Rev. Mater. Sci.*, vol. 16, p. 163, 1986.
Horwitz, C. M.: *J. Vac. Sci. Technol.*, vol. A1, p. 90, 1983.
Kemper, M. J. H., S. W. Koo, and F. Huizinga: in G. S. Mathad *et al.* (eds.), *Plasma Processing*, The Electrochemical Society, Pennington, N.J., 1985.
Kettani, M. A., and M. F. Hoyaux: *Plasma Engineering*, Wiley, New York, 1973.
Langmuir, I.: *General Electric Rev.*, vol. 26, p. 731, 1923.
——— and H. Mott-Smith: *General Electric Rev.*, vol. 27, pp. 449, 538, 616, 762, 810, 1924.
Ligenza, J. R.: *J. Appl. Phys.*, vol. 36, p. 2703, 1965.
Maissel, L.: in L. Maissel and R. Glang (eds.), *Handbook of Thin Film Technology*, chap. 4, McGraw-Hill, New York, 1970.
Meyerson, B. S., E. Ganin, D. A. Smith, and T. N. Nguyen: *J. Electrochem. Soc.*, vol. 133, p. 1232, 1986.
Mogab, C. J., A. C. Adams, and D. L. Flamm: *J. Appl. Phys.*, vol. 49, p. 3769, 1978.
Morgan, R. A.: *Plasma Etching in Semiconductor Fabrication*, Elsevier, London, 1985.
Nguyen, V. S., J. Underhill, S. Fridmann, and P. Pan: in G. S. Mathad *et al.* (eds.), *Plasma Processing*, The Electrochemical Society, Pennington, N.J., 1985.
Petro, W. G., B. R. Cairns, and K. V. Anand: in H. Huff *et al.* (eds.), *Semiconductor Silicon 1986*. The Electrochemical Society, Pennington, N.J. 1986.
Steinbruchel, C.: *J. Vac. Sci. Technol.*, vol. A3, p. 1913, 1985.
Sugiura, H., and M. Yamaguchi: *Jap. J. Appl. Phys.*, vol. 19, p. 583, 1980.
Tu, Y. Y., T. J. Chuang, and H. F. Winters: IBM Research Report RY 2810, 1981.
Turban, G.: *Pure and Appl. Chem.*, vol. 56, p. 215, 1984.
Vratny, F.: *J. Electrochem. Soc.*, vol. 114, p. 505, 1967.
Wehner, G. K., and G. S. Anderson: in L. Maissel and R. Glang (eds.), *Handbook of Thin Film Technology*, chap. 3, McGraw-Hill, New York, 1970.

CHAPTER 10

PHYSICAL VAPOR DEPOSITION APPARATUSES AND PLASMA REACTORS

10.1 INTRODUCTION

Apparatuses and reactors used for physical and physicochemical processes are diverse. They range from vacuum deposition apparatuses, sputtering equipment, elaborate molecular beam epitaxy (MBE) apparatuses, and various types of plasma reactors. Physical sputtering and MBE are the principal physical vapor deposition (PVD) processes. Physical sputtering remains a major method of metallization in which metals are deposited. MBE is the preferred choice for epitaxial deposition of thin films of III-V compounds, particularly when heterostructures with sharp doping profiles are desired. Any apparatus for PVD requires an elaborate vacuum system.

The phenomena taking place in a plasma reactor are quite complex. The added complications, compared to conventional CVD reactors, arise from the presence of plasma, a medium that literally determines the fate of deposition or etching. At the core of the complications are the collision processes in plasma leading to the formation of electrons, ions, and reactive neutral species, the transport phenomena within the plasma and in the sheaths, and their relation to the

Gorowitz, B., T. B. Gorezyea, and R. J. Saia: *Solid State Technol.*, p. 179, June 1985.
Greene, J. E., and S. A. Barnett: *J. Vac. Sci. Technol.*, vol. 21, p. 285, 1982.
Harper, J. M. F., J. J. Cuomo, P. A. Leary, G. M. Summa, H. R. Kaufmann, and F. J. Bresnock: *J. Electrochem. Soc.*, vol. 128, p. 1077, 1981.
Hasted, J. B.: *Physics of Atomic Collision*, Butterworth, London, 1964.
Hess, D. W.: *Ann. Rev. Mater. Sci.*, vol. 16, p. 163, 1986.
Horwitz, C. M.: *J. Vac. Sci. Technol.*, vol. A1, p. 90, 1983.
Kemper, M. J. H., S. W. Koo, and F. Huizinga: in G. S. Mathad *et al.* (eds.), *Plasma Processing*, The Electrochemical Society, Pennington, N.J., 1985.
Kettani, M. A., and M. F. Hoyaux: *Plasma Engineering*, Wiley, New York, 1973.
Langmuir, I.: *General Electric Rev.*, vol. 26, p. 731, 1923.
——— and H. Mott-Smith: *General Electric Rev.*, vol. 27, pp. 449, 538, 616, 762, 810, 1924.
Ligenza, J. R.: *J. Appl. Phys.*, vol. 36, p. 2703, 1965.
Maissel, L.: in L. Maissel and R. Glang (eds.), *Handbook of Thin Film Technology*, chap. 4, McGraw-Hill, New York, 1970.
Meyerson, B. S., E. Ganin, D. A. Smith, and T. N. Nguyen: *J. Electrochem. Soc.*, vol. 133, p. 1232, 1986.
Mogab, C. J., A. C. Adams, and D. L. Flamm: *J. Appl. Phys.*, vol. 49, p. 3769, 1978.
Morgan, R. A.: *Plasma Etching in Semiconductor Fabrication*, Elsevier, London, 1985.
Nguyen, V. S., J. Underhill, S. Fridmann, and P. Pan: in G. S. Mathad *et al.* (eds.), *Plasma Processing*, The Electrochemical Society, Pennington, N.J., 1985.
Petro, W. G., B. R. Cairns, and K. V. Anand: in H. Huff *et al.* (eds.), *Semiconductor Silicon 1986*. The Electrochemical Society, Pennington, N.J. 1986.
Steinbruchel, C.: *J. Vac. Sci. Technol.*, vol. A3, p. 1913, 1985.
Sugiura, H., and M. Yamaguchi: *Jap. J. Appl. Phys.*, vol. 19, p. 583, 1980.
Tu, Y. Y., T. J. Chuang, and H. F. Winters: IBM Research Report RY 2810, 1981.
Turban, G.: *Pure and Appl. Chem.*, vol. 56, p. 215, 1984.
Vratny, F.: *J. Electrochem. Soc.*, vol. 114, p. 505, 1967.
Wehner, G. K., and G. S. Anderson: in L. Maissel and R. Glang (eds.), *Handbook of Thin Film Technology*, chap. 3, McGraw-Hill, New York, 1970.

CHAPTER 10

PHYSICAL VAPOR DEPOSITION APPARATUSES AND PLASMA REACTORS

10.1 INTRODUCTION

Apparatuses and reactors used for physical and physicochemical processes are diverse. They range from vacuum deposition apparatuses, sputtering equipment, elaborate molecular beam epitaxy (MBE) apparatuses, and various types of plasma reactors. Physical sputtering and MBE are the principal physical vapor deposition (PVD) processes. Physical sputtering remains a major method of metallization in which metals are deposited. MBE is the preferred choice for epitaxial deposition of thin films of III-V compounds, particularly when heterostructures with sharp doping profiles are desired. Any apparatus for PVD requires an elaborate vacuum system.

The phenomena taking place in a plasma reactor are quite complex. The added complications, compared to conventional CVD reactors, arise from the presence of plasma, a medium that literally determines the fate of deposition or etching. At the core of the complications are the collision processes in plasma leading to the formation of electrons, ions, and reactive neutral species, the transport phenomena within the plasma and in the sheaths, and their relation to the